RESEARCH PAPER

Evaluation of *In vivo* Anti-inflammatory Activity and Characterization of Iron Nanoparticles Biogenically Synthesized using *Ocimum tenuiflorum* leaf extract

Anshul Sharma[1], Manjeet Kaur[2]*

[1,2*] Department of Biotechnology, University Institute of Engineering and Technology, Maharshi Dayanand University, Rohtak-124001, Haryana, India

anshulsharma.7293@gmail.com , manjeetkaurbiotech.uiet@mdurohtak.ac.in

Abstract

The present study reports the green synthesis of iron nanoparticles (INPs) using *Ocimum tenuiflorum* (Tulsi) leaf extract in 20% ethanol and their evaluation for anti-inflammatory activity. The characterization was done by UV-Vis spectroscopy, Fourier transform infrared (FTIR) spectroscopy, scanning electron microscopy (SEM), transmission electron microscopy (TEM) and X-Ray diffraction (XRD). The anti-inflammatory activity of INPs was assessed through both in vitro and in vivo models. In vitro HRBC assays demonstrated significant inhibition, comparable to that of the standard anti-inflammatory drug diclofenac. In vivo anti-inflammatory efficacy was evaluated in mice using EPP and carrageenan-induced paw edema assays. The INP-treated groups showed a significant reduction in ear and paw edema, with efficacy comparable to that of diclofenac. Additionally, in vitro and in vivo biocompatibility studies confirmed the non-toxic nature and biological safety of the synthesized INPs. The results of this study suggest that *O. tenuiflorum*-mediated iron nanoparticles exhibit promising anti-inflammatory properties and good biocompatibility, indicating their potential as a novel and effective therapeutic agent for inflammatory disorders.

Key word: Iron nanoparticles, *Ocimum tenuiflorum*, characterization, anti-inflammatory activity.

How To Cite This Article: Sharma A, Kaur M. Evaluation Of In Vivo Anti-Inflammatory Activity And Characterization Of Iron Nanoparticles Biogenically Synthesized Using Ocimum Tenuiflorum Leaf Extract. Int J Drug Deliv Technol. 2026;16(27s):654-666. Doi: 10.25258/ijddt.16.27s.75

Introduction

Iron nanoparticles (INPs) are incredibly small particles with nanoscale dimensions that can be prepared by physical, chemical, and biological methods [1]. Among these methods, biological synthesis using microorganisms and plant extracts is preferred, as it is non-toxic, cheaper, and eco-friendly for the synthesis of INPs with superior properties [2,3]. The main shortcoming of microbial-dependent INP synthesis exercises is the need to maintain sterile conditions, which requires highly trained staff and also increases the cost of scaling up [4]. INPs of a variety of shapes and sizes have been synthesized using the plant extracts of an array of angiosperms [5]. *Ocimum tenuiflorum,* generally known as 'Tulsi', belongs to the family Lamiaceae and is native to India and Southeast Asia. Its extract has been used in traditional Ayurvedic medicine due to its potential for treating and preventing many diseases [6,7]. Anti-inflammatory and analgesic activity of O. sanctum was attributed to various phytochemicals present in its different parts [8-10]. *O. tenuiflorum* has exhibited good anti-bacterial, anti- inflammatory, anti-oxidant, and anthelmintic activity [11, 12]. There are various studies on phyto-synthesis of INPS using leaf extract of *O. tenuiflorum* [13-17]. INPs should be characterized for size, shape, stability, and structure prior to their intended applications in fields such as agriculture, bioengineering, biomedical, biotechnology, environment, medical, and therapeutics [5]. This characterization can be done by UV-Vis spectroscopy, FTIR spectroscopy, zeta potential, SEM, TEM and X-XR-D.

Inflammation

Inflammation is a typical physiological response to pathogens and tissue injury, and by initiating pathogen-killing and tissue repair processes, it helps restore homeostasis at infected or damaged sites. It's characterized by erythema, edema, heat, discomfort, and loss of function, and is brought on by interactions among several cell types, as well as the production and reactions to a wide range of chemical mediators. Inflammatory responses need to be managed to maintain health and homeostasis [18]. According to recent research, inflammation may be present in a broader range of disorders [19]. Anti-inflammatory medications now on the market come with a variety of adverse effects, including indigestion, fluid retention, and issues with kidney, liver, and heart function. [20, 21]. There is a variety of nanoparticles that display anti-inflammatory action via different mechanisms. However, there is no scientific investigation on the *in vivo* anti-inflammatory action of INPs.

Halloysite, a naturally occurring clay mineral, was found to contain iron in the form of Fe+3 and a small domain of magnetically arranged ferrihydrite approximately 3 nm in size. The anti-inflammatory response was demonstrated by early inhibition of

*Author for Correspondence: manjeetkaurbiotech.uiet@mdurohtak.ac.in

edema by halloysite and by treated halloysite possessing labile iron. Iron present in aqueous or nanoparticulate form can be utilized by leukocytes or precipitated by them, and thus, natural Fe-halloysite affected the infiltration of these inflammatory cells [22]. Green-synthesized silver, gold, and zinc nanoparticles have shown strong anti-inflammatory activity [23]. Silver nanoparticles (Ag NPs) biosynthesized using *Viburnum opulus*, with an average size of 25 nm and spherical shape, have shown in vitro and in vivo anti-inflammatory activity. The Ag NPs have inhibited the secretion of interleukins 1 and 6 and reduced carrageenan-induced paw edema, demonstrating anti-inflammatory activity in vitro and in vivo, respectively [24]. The anti-inflammatory mechanism of Zinc oxide nanoparticles (ZnO NPs) contributes to the downregulation of inflammatory marker genes IL-1β, IL-6, IL-10, TNF-α, and COX-2. ZnO NPs interacted with various serum proteins, forming a protein corona via adsorption, thereby affecting the immune response, hindering myeloperoxidase activity, and altering cytokine secretion. [25]. Crystalline magnesium oxide nanoparticles (MgONPs) with a size of 19.57 nm have been prepared using *Alstonia scholaris* leaf extract. MgONPs have shown higher antioxidant and anti-inflammatory activity than ascorbic acid and diclofenac sodium, respectively [26]. Selenium nanoparticles synthesized from the aqueous extract of *Polycladia crinite*, a brown alga, have been characterized and found to exhibit dose-dependent antioxidant and anti-inflammatory effects [27]. ZnO NPs of 31 nm average size and crystalline structure, synthesized using leaf extract of *Senecio chrysanthemoides*, have been reported to exhibit higher anti-inflammatory activity than diclofenac sodium [28]. Anti-inflammatory properties of AgNPs and ZnO NPs synthesized using *O. tenuiflorum* and *Ocimum gratissimum* extract have been reported to be comparable to diclofenac sodium [29]. *Aphania senegalensis* leaf extract has been employed for the preparation of AgNPs with average diameters of 18.11-50 nm, exhibiting 10 times higher anti-inflammatory activity than the leaf extract [30].

Nanoparticles' biocompatibility can be assessed by cytotoxicity assays, in vitro using cell lines and in vivo using animal models [31-34]. Bio-compatibility of INPs was measured by a hemolysis assay [35]. In vivo toxicity of INPs can be analyzed by using animal models [36-40]. Zebrafish are increasingly accepted as a contemporary experimental animal model worldwide. In the domain of toxicological and biological testing, this animal model is gaining ground during the adult and developmental stages. There is high-level genome homology between zebrafish and humans, making it an animal model for toxicity analysis [41, 42]. The present study is focused on the characterization of biogenically synthesized INPs using *O. tenuiflorum* leaves extract and the assessment of their anti-inflammatory action. Further, assessment of biocompatibility along with the toxicity of synthesized INPs has been done.

Materials and Methods

Plant Collection and Preparation of Extract

The collection of *O. tenuiflorum* leaves and the preparation of extracts were performed as previously reported by our research team [43, 44].

Biogenic Synthesis of Iron Nanoparticles

Biogenic synthesis of INPs and collection of as-synthesized INPs were carried out as described by Sharma *et al*. (2025). [43]

Characterization of Synthesized INPs

Several techniques, such as UV-Vis spectroscopy, FTIR spectroscopy, zeta potential analyzer, SEM and TEM, Particle size analyzer, and X-ray diffraction (XRD), were used to characterize the synthesized INPs.

UV-Vis Spectroscopy: Analysis of the optical wavelength of INPs was performed using a UV-Vis spectrophotometer (Shimadzu UV-3600i Plus). UV-vis spectra of manufactured INPs were noted between 200-800nm. The shape, size, and stability of synthesized NPs correspond to the specific peak position of surface plasmon resonance of NPs.

FT-IR Spectroscopy: It is a method for recording infrared spectra. FTIR spectra of synthesized INPs were recorded from 500-4000cm^{-1}, to identify the type of bond and functional groups present.

Zeta-Potential Analysis: The stability of INPs was checked by measuring their zeta potential. The zeta potential of synthesized INPs was calculated using Zeta sizer Instrument (Malvern Instruments Ltd.) at Aryabhata Centralized Laboratory, MDU Rohtak.

Particle Size Analysis:

SEM: SEM images exhibit a significant depth of field, giving a characteristic 3D appearance that is helpful for understanding nanoparticle morphology. SEM was used to study the morphology of synthesized INPs. It was carried out at the Raman & XRD Central Instrumental Laboratory (CIL), GJU, Hisar.

TEM: TEM of synthesized INPs was done as reported earlier by Sharma *et al* (2025).

X-Ray diffraction (XRD): XRD analysis carried out for INPs was as stated by Sharma *et al*, 2025. [43]

Anti-inflammatory Activity of Synthesized INPs

***In-vitro* Anti-inflammatory assay:** The Human red blood cell (HRBC) stabilization experiment was performed to analyze the *in vitro* anti-inflammatory activity of INPs. Fresh blood was collected and transferred in EDTA vacationer in order to avoid coagulation. The blood was added to a similar amount of sterile Alsever's solution (2.05% dextrose, 0.8% sodium citrate, 0.055% citric acid, and 0.42% sodium chloride in 100 milliliters of distilled water). After thorough mixing, it was centrifuged at 3000 rpm for 15 minutes. The supernatant was removed, and pellets were used for further experimentation. The HRBC pellet was kept at 4 °C for approximately 24 hours prior to the experiment and rinsed three times with iso-saline

solution. The iso-saline solution was used to prepare 10% HRBC suspension. This HRBC suspension was used to estimate *in vitro* anti-inflammatory activity. 100, 150, and 200 µg/ml of biogenically synthesized nanoparticles, diclofenac as a reference drug, and control were each mixed with 1.0 ml of phosphate buffer, 2 ml of hyposaline, and 0.5 ml of HRBC suspension. All testing mixtures were kept at 37 °C for 30 minutes prior to centrifugation at 3000 rpm. The supernatant was collected, and absorbance was measured at 560 nm using a spectrophotometer. The percentage hemolysis was calculated by supposing that the hemolysis developed in the control would be 100%. The percentage of hemolysis of the HRBC membrane was noted as follows by taking equation no. 1: [44, 45]

% Hemolysis = Optical density of Test sample X 100 Eq. (1)
Optical density of Control

The estimated percentage of HRBC membrane stabilization was act in accordance with:

% Protection = 100 – % of hemolysis

Nanogel/ INPs Nano formulation preparation

5 g of INPs was gently mixed with 5 mL of *O. tenuiflorum* oil and 5 mL of glycerol for 15 min to form a uniform dispersion. To further assess *in vivo* anti - inflammatory activity of INPs this nano formulation of 0.5g/ml concentration was used for topical application.

***In-vivo* Anti-inflammatory Activity Assay**

For this investigation, white albino mice of 25-35 g weight were kept in a normal polypropylene cage at room temperature (22°C–24°C) during the 12:12-hour light/dark cycle. The mice were procured from the Disease Free Small Animal House, Lala Lajpat Rai University of Veterinary and Animal Sciences, Hisar. During their 6-week acclimatization, they were supplied with regular pellet food and water ad libitum. The experiments have been duly approved by the Institutional Animal Ethics Committee, Maharshi Dayanand University, Rohtak, and all studies were conducted in accordance with it vide letter no. CAH/23/5-12 Dated 19-01-23.

Ethyl phenyl propiolate (EPP) Induced Ear Edema Test- The EPP ear edema test is a frequently used method to determine a substance's anti-inflammatory activity. Male mice (weighing between 25 and 35g) were divided into four groups (n=6). Both the inner and outer surfaces of the right ear were inflamed by topically applying 1 mg/20 µl/ear of EPP. At 0, 60, 120, 180, and 240 minutes after edema induction, the thickness of both ears was measured with a vernier caliper. Topical application of the nanoformulation of INPs was applied to the test groups; water to the control; and diclofenac gel, an anti-inflammatory drug, to the reference groups. At each recording interval, the outcomes of in vivo anti-inflammatory interventions were analyzed and compared with those of the control group. [46]

Carrageenan Persuade Paw Edema Model: *In vivo* anti-inflammatory action of synthesized INPs was assessed by employing carrageenan- induced paw edema in mice as stated by the accepted protocol described by Winter *et al*., 1962. Male mice were divided into a set of three groups (n=6). The basal volume of the right hind paw of each and every mouse was measured prior to the execution of carrageenan by using a plethysmometer. Edema was induced by applying 0.05 ml of a freshly prepared 1% carrageenan solution in normal saline to the left hind paw of each mouse in all assembled groups. The shift in volume of each test paw, indicating inflammation, was measured at 1, 2, 3, and 4 hours after carrageenan application. The average inflammation in INPs acted mice, along with the standard, was set side by side with the negative control. The percent inhibition of edema (anti-inflammatory) was determined using equation no. 2. [47]

% Inhibition of edema =Co − Ct /Co × 100. Eq. (2)

Where Co is the average inflammation of the control group at a stated time, and Ct is the average inflammation of INP-actuated mice at the same time.

Biocompatibility and Toxicity study of Synthesized Iron Nanoparticles

Hemocompatibility: To assess hemocompatibility, hemolysis of human red blood cells was evaluated. Fresh blood was collected in an EDTA tube to prevent coagulation. The blood sample was centrifuged by SpinWin at 10000 rpm for 10 minutes. Red blood cells were isolated from the plasma and white blood cells in the blood sample. The obtained RBCs were washed with 10 mM phosphate-buffered saline (PBS, pH 7.2) and diluted to 5% (v/v). Then, 50 µL of RBC were mixed with 100, 150, and 200 µg/mL of INPs, and the mixture was incubated for 1 hour at 37 °C with shaking at 150rpm. RBCs were incubated with 10Mm PBS (pH 7.2) for the negative control experiment and 0.1% sodium carbonate for the positive control experiment, respectively. After incubation, the solution was centrifuged at 2500 rpm for 5 minutes, and 100 µL of the supernatant was then transferred to a 96-well plate. The percentage of hemolysis was estimated utilizing the equation no. 3 below. The value of absorbance of the supernatant was determined at 545 nm with a microplate reader. Hemolysis percentage was determined using the subsequent relationship:

$$\%\text{Hemolysis}=\frac{A_{Sample}-A_{Negative}}{A_{Positive}-A_{Negative}}\times 100 \quad \text{Eq. (3)}$$

Toxicity Study: The survival of zebra fish exposed to 100 to 200 micro g mL−1 concentrations of synthesized INPs was determined at specific time intervals from 48 - 168 hrs. Toxicity was measured using a mortality assessment method. Acute nanoparticle exposure increases the risk of developing a critical disease and the mortality rate. As previously mentioned, zebrafish have a number of benefits, but from the standpoint of environmental and human safety (EHS), they are a

special model. The data generated by nano EHS research can help reduce the risks associated with nanomaterials and nanotechnology-related products in the near future. The data may also help us formulate sensible criteria for safety precautions, quality assurance, and design strategies to enhance nanomaterials and reduce toxicity.

Results and Discussion

Results

Characterization of Synthesized INPs

The black colored INPs were harvested as reported by our research team [43]. This formation of INPs is consistent with earlier findings from our lab [44] and with previous reports on IONP formation [48-51]. On GCMS analysis of *O. tenuiflorum* phytochemicals and density functional calculation of these phytochemicals with iron ions, it has been found that two molecules of 1,16-cyclocoryan-17-oic acid-19,20-didehydro-methyl ester made a stable bond with Fe2+, with higher interaction energy, indicating a major role of this phytochemical in the formation and stabilization of INPs. While one methyl eugenol molecule weakly bonded with Fe2+ by van der Waals interactions [43]. This INP formation mechanism study can be further established by exploring the use of purified phytochemicals of *O. tenuiflorum* for INP synthesis.

UV-VIS Spectroscopy: The absorption spectra of biogenically synthesized INPs recorded between 200-800nm are presented in Figure 1. The surface plasmon resonance broad peak is in the range of 370 to 400 nm due to vibrational excitations in INPs. An absorption peak at 374.5nm was observed, indicating the formation of INPs. Our results are similar to those reported in earlier research [52, 53]. The absorption peak at 270 nm has been reported for iron oxide nanoparticles synthesized using *Camellia sinensis* extracts [54]. Some studies outlined the presence of INPs at 405 nm [55, 56]. Earlier investigations have documented that the peak at 371.1 corresponds to iron oxide nanoparticles [57]. Some researchers have documented that INPs exhibited an absorption peak between 280 and 420 nm [58, 59]. Phytochemicals are the major contributors to the formation and stabilization of INPs [60].

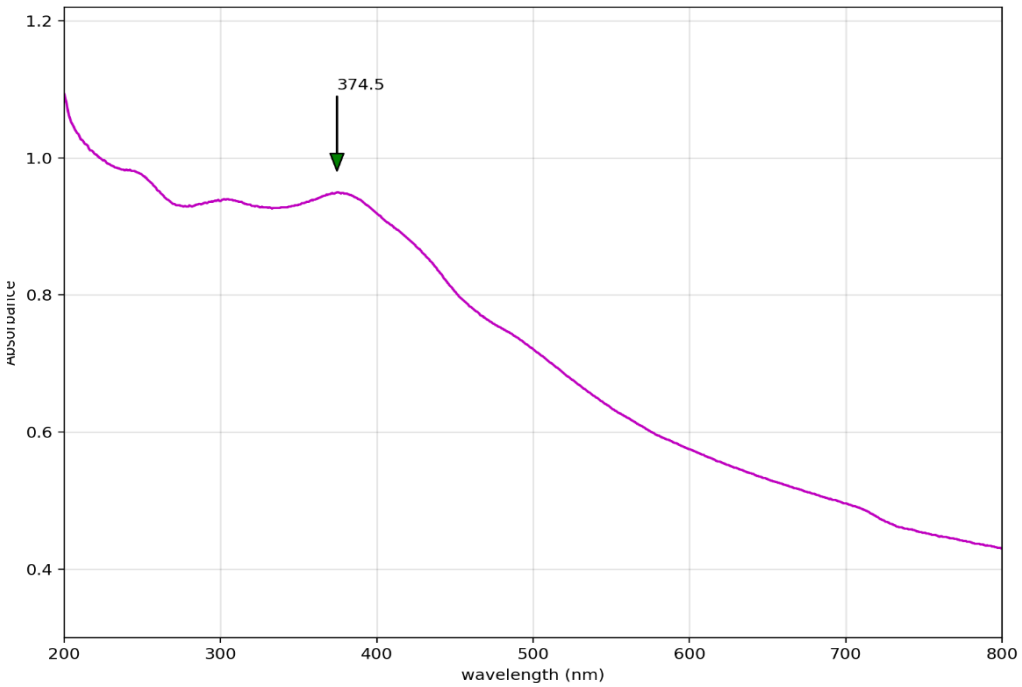

Fig.1. UV-Vis spectra of synthesized INPs.

FT-IR Spectroscopy: The functional groups and types present and involved in the reduction, capping, and stabilization of INPs were detected from chemical bond excitations revealed by FTIR spectra of synthesized INPs. The interaction between reducing agents, capping agents, and INPs was represented in terms of wavenumbers [61]. The FTIR analysis of INPs in Figure 2 showed the peaks at 536.60, 563.60, 607.95, 578.55, 1625.72, 2097.24, 3286.16, and 3232.64. The peak at 536.60, 563.60, 607.95 was due to the presence of alkyl halide, peak at 1625 stands for N-H bend of primary amines, 2097 stands for alkynes --C≡C-, 3286.16 stands for -C≡C-H: C-H stretch alkynes (terminals), peak at 3232.64 stands for OH stretch, H-bond (depicting the presence of alcohols and phenols) and O-H stretch of carboxylic group. These functional groups would have played a significant role in the synthesis and stabilization of INPs. The various peaks present in FTIR spectra of INPs are an indication that *O. tenuiflorum* extract's phytochemicals served as

reducing, capping, and stabilization agents in biogenic synthesis of INPs. It has been reported in earlier research that the different types of IONPs can show peaks at 470, 501 to 633 cm-1 wavenumbers [62, 63]. The specific peaks observed are due to extract of particular type of plant, geographical location, cultivation methods and extraction process employed.

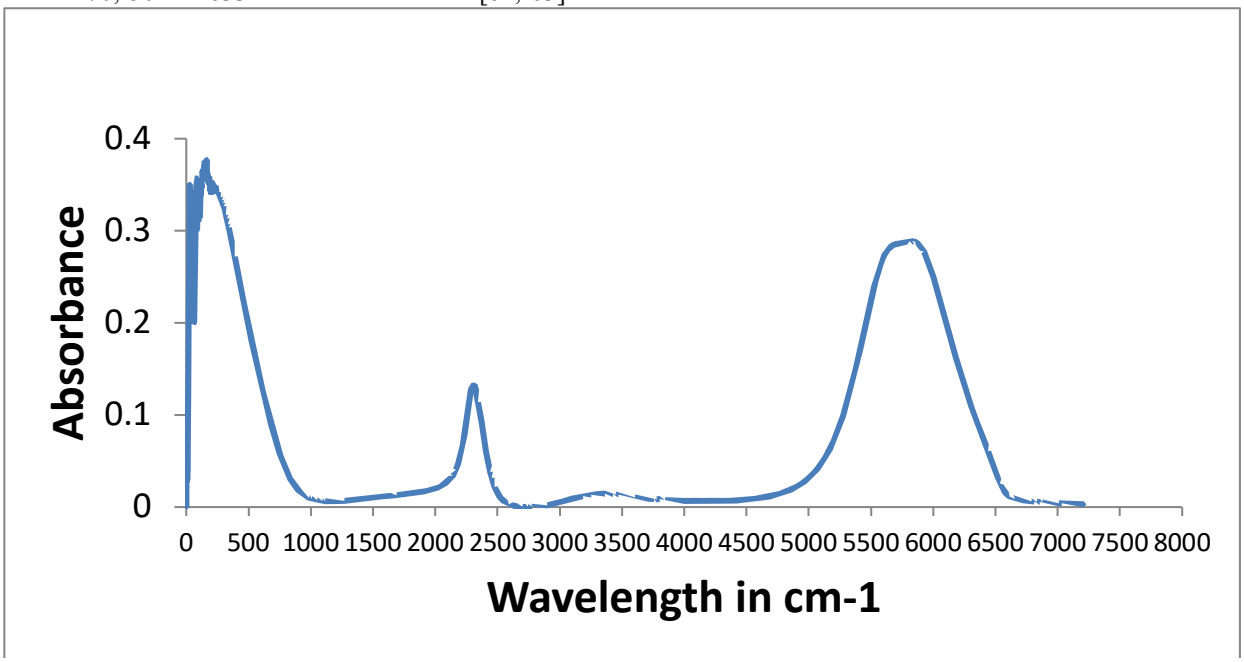

Fig.2. FTIR spectra of synthesized INPs.

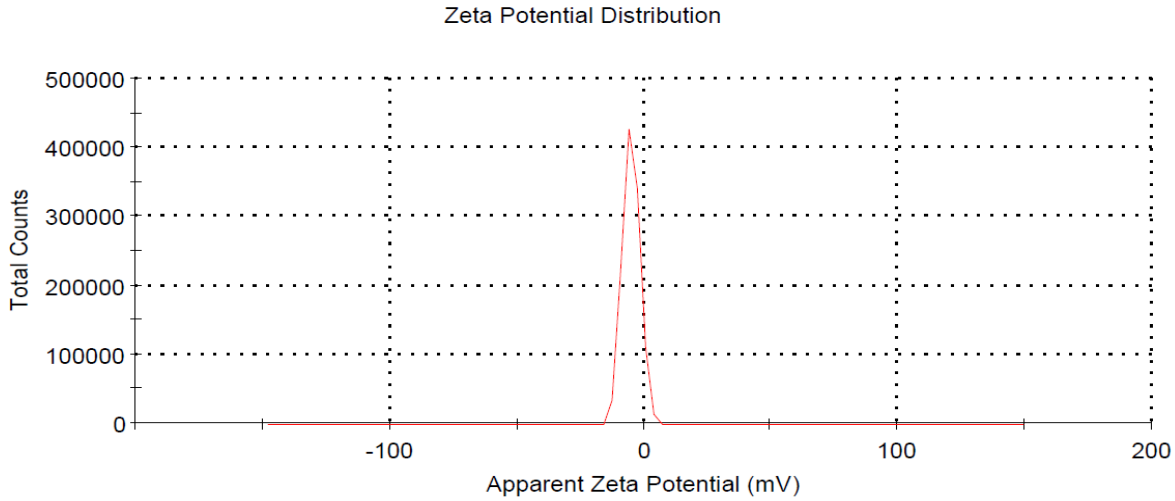

Fig.3. Zeta potential of synthesized INPs.

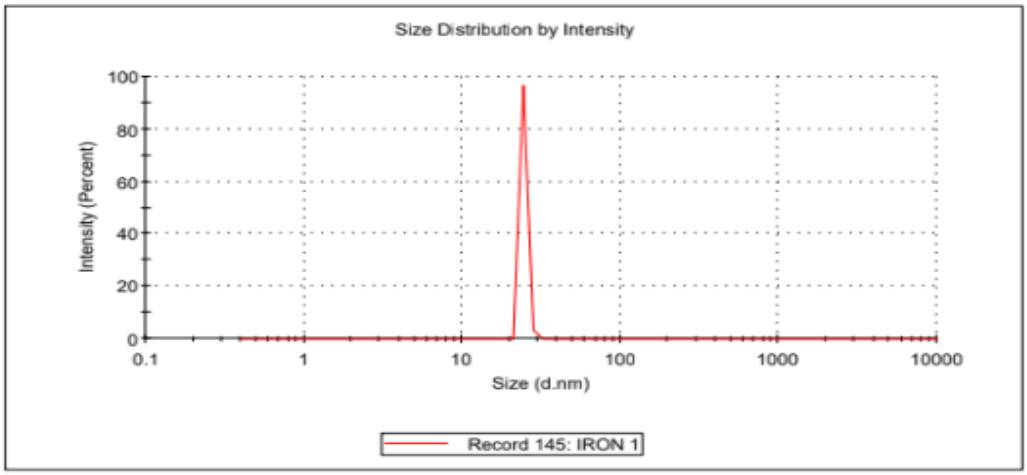

Fig.4. Size distribution by intensity INPs synthesized using *O.tenuiflorum* leaf extract.

Zeta potential analyzer was used to observe the surface potential of INPs for assessment of their stability in solution and zeta potential of INPs is shown in Figure 3. Nanoparticles are regarded steady if zeta potential values are either more than +30 mV or more than -30 mV [64]. Generally, Zeta potential value of 35 mV is theoretical limit for stable nanoparticles in suspension form [65]. Zeta potential of INPs was noticed to have value of -4.92 mV and it is indicating the formation of highly stable nanoparticles. Our results are nearly similar to previous reported research [66] and contradictory to research study [67]. Figure 4 shows size distribution of INPs on X- axis and intensity of scattered light on Y -axis. A sharp peak was observed indicating the uniform size distribution of nanoparticles. The size distribution of synthesized INPs observed was 50- 70 d.nm. In Figure 5 SEM images show the surface structure of synthesized INPs. It can be noticed that nanoparticles are of spherical to irregular granular shaped. The presence of cover on INPs depicted their capping done by capping agents and stabilizing agents' role being displayed by phytochemicals of *O. tenuiflorum* leaf extract. Our findings match to previous research study [48, 49, 66, 69]**.** INPs got agglomerated to form larger particles of undefined shape and it can be attributed to presence of phytochemicals on nanoparticles surface [70, 71]. Aggregation of nanoparticles have been reported by other researchers [51].

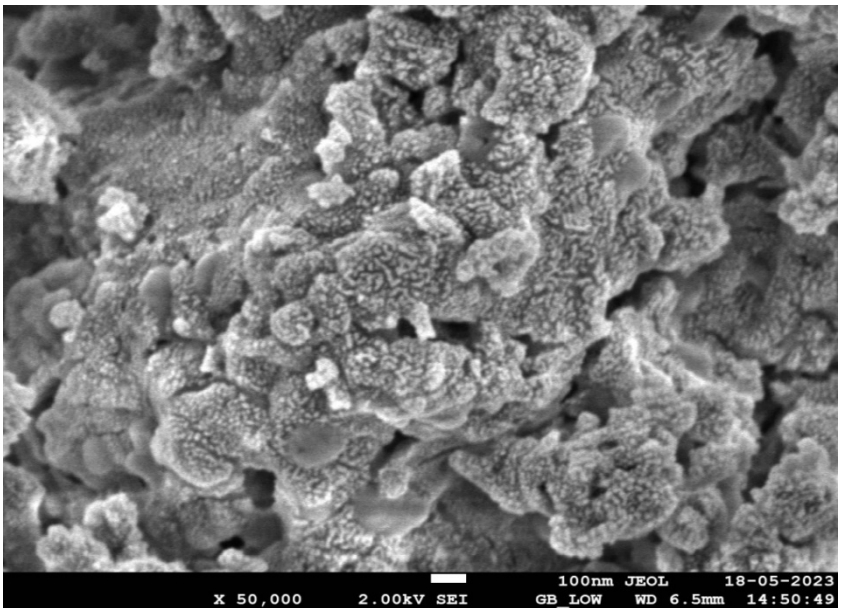

Fig.5. SEM image of synthesized INPs.

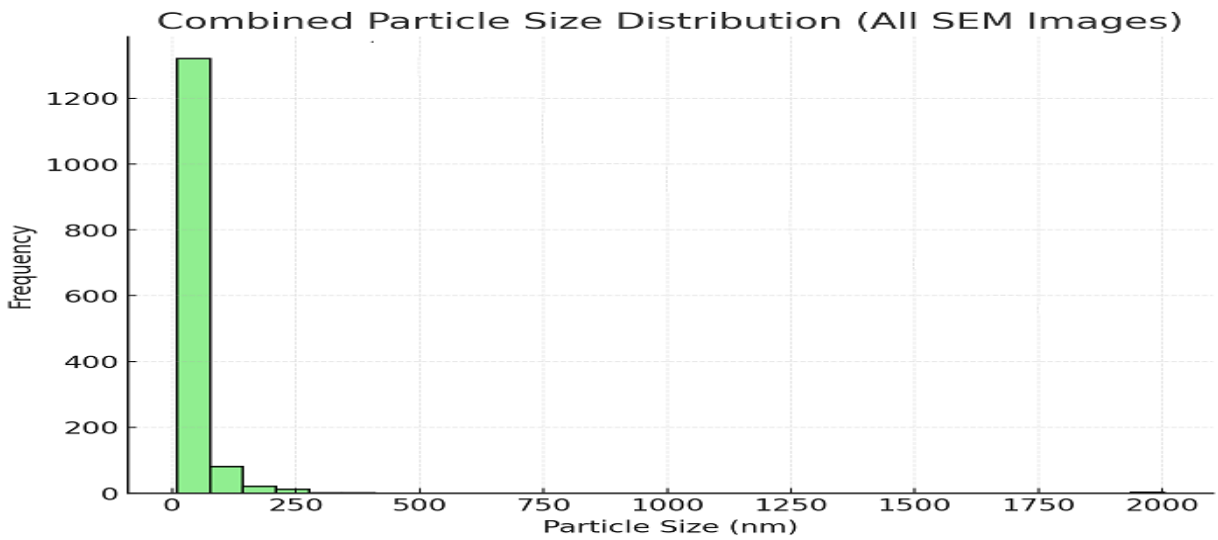

Figure 6 Histogram of diameter range of INPs.

Figure 6 represents a histogram of the diameter range of INPs. The diameter range of nanoparticles was observed between 9.64 and 2002.5 nm with an average size of 42.27 nm. Nanoparticles with a diameter of 42 nm can serve as anti-inflammatory agents and as ideal drug delivery agents [72]. A histogram of the nanoparticle sizes was designed by software of OriginPro data analysis.

Transmission electron microscope reveals the size of nanoparticles formed. TEM is a major analytical method in the physical and biological sciences. TEM of iron nanoparticles in Figure 7 showed that the majority of spherical-shaped INPs of 50nm are formed. Our results coincide with other study [51, 73, 74]

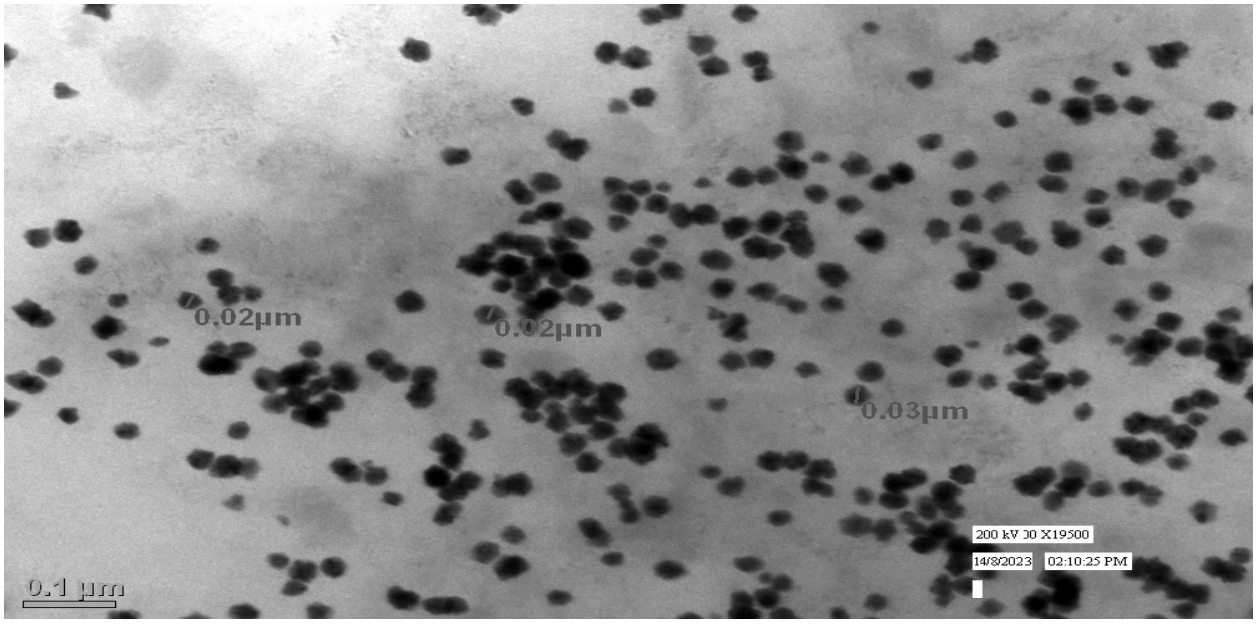

Fig.7. TEM image of synthesized INPs.

XRD peaks at 41.22 and 29.76 in Figure 8 shows that the nanoparticles formed were crystalline in nature and formation of Iron nanoparticles takes place.

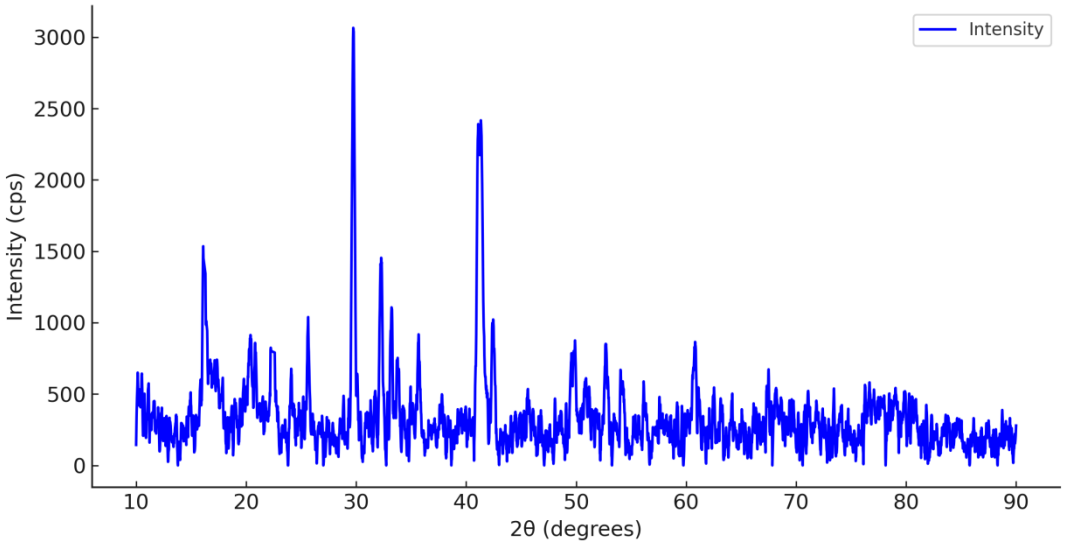

Fig.8. XRD image of synthesized INPs.

***In vitro* Anti-inflammatory action of Synthesized INPs**

The biogenically obtained iron NPs concentration-dependent anti-inflammatory properties were examined. All the observed data are presented in Figure 9. The synthesized INPs show most significant percentage membrane stabilization of 37.69, 49.90, 58.30 % in compare of diclofenac 18.60, 27.19, 37.78 % on 100, 150 and 200 µg/ml respectively. According to these findings, biogenically synthesized INPs have anti-inflammatory properties and effectively reduce inflammation in human red blood cell. Biogenically synthesized INPs from *O. tenuiflorum* may be a therapeutic possibility against inflammatory illnesses by lowering according to our initial in vitro anti-inflammatory investigations.

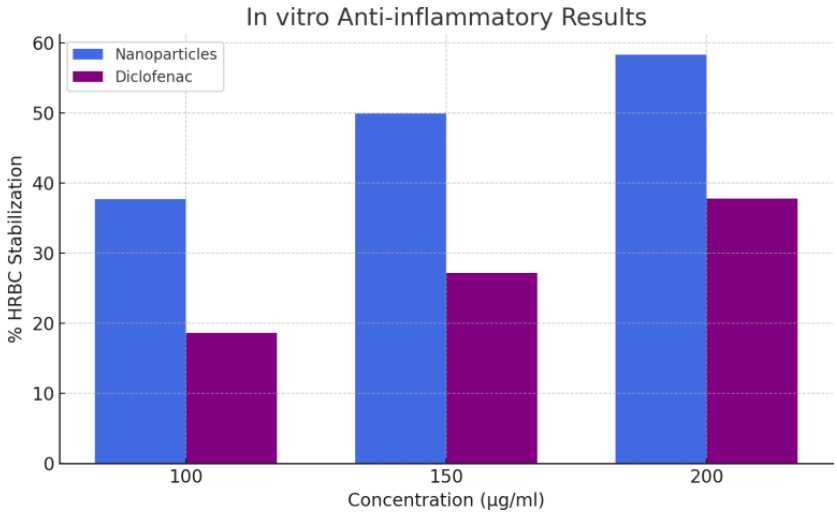

Fig.9. In vitro anti- inflammatory results having a comparison between INPsand standard drug, diclofenac.

***In vivo* Anti-inflammatory activity of Synthesized INPs**

EPP Assay

Outcomes received from EPP-induced albino mice ear edema are illustrated in Figure 10. Iron nanoparticles at the dose of 1 mg per ear inhibited the edema formation notably. The percentage inhibition noted was 11.76, 20.30, 29.30, 33.55 and 40.55 % when measurement was made at 40, 80, 120, 160 and 200 min succeeding application of EPP. The diclofenac at the dose of 4 mg per ear considerably inhibited the ear edema formation with percentage inhibition of 10.96, 23.27, 29.60, 35.31 and 37.81 at 40, 80, 120, 160 and 200 min, respectively. The green synthesized INPs markedly inhibited ear edema formation induced by EPP. It is proposed that the green synthesized iron nanoparticles from *O. tenuiflorum* in all probability has anti-inflammatory actions like diclofenac, by means of inhibition of the inflammatory arbitrators of the sharp stage of inflammation.

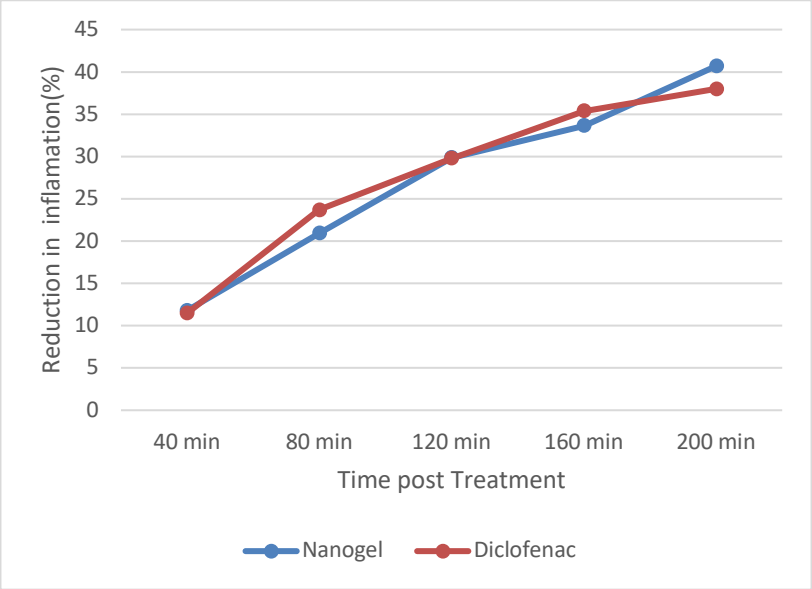

Fig.10. In vivo anti- inflammatory results having a comparison between nanogel and standard drug diclofenac using EPP-induced albino mice ear edema assay.

Paw edema test

The anti-inflammatory effect of INPs obtained by the leaf extract of *O. tenuiflorum* on carrageenan-induced edema in the hind paw of mice was examined. There was no lowering of inflammation in the control group mice. The outcomes in Figure 11 indicate that iron nanoparticles significantly reduce inflammation at a 100 mg/kg dose, comparable to a standard anti-inflammatory drug.

The percentage inhibition in paw volumes of each group after carrageenan administration with iron nanoparticles was 24.72, 34.72, 28.22, and 35.83 % at 40, 80, 120, and 160 min after applying EPP, respectively. The diclofenac at a dosage of 4 mg per ear inhibited ear edema, with % inhibition of 17.08, 22.03, 22.69, and 30.92 at 40, 80, 120, and 160 min, respectively.

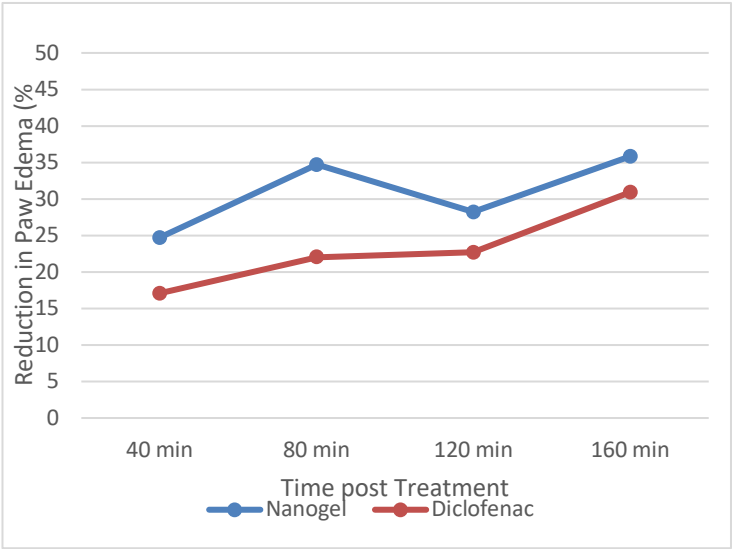

Fig.11. In vivo anti- inflammatory results showing a comparison between nanoparticles and the standard drug diclofenac using carrageenan-induced edema in the hind paw of mice.

Biocompatibility assay of Synthesized INPs

The absorbance parameters of supernatant liquids treated with 100, 150, and 200 µg /ml concentrations was assessed and analysed with the results of ruptured RBCs in a suspension of deionized water (taken as 100% lysed, negative control) and blood in PSS buffer devoid of any INPs (taken as 0% lysed, positive control), using Eq. (3). Considering ISO 10993-4 standard for evaluating biological medical devices satisfactory for blood contact, the constituent

substances should possess haemolysis rates that are less than 5% [75]. In the current investigation, hemolysis rates were less than 2% at all assessed concentrations. The value was 01 ± 0.73% for low nanoparticle content (17.4 µg (Fe3O4)/mL) and 1.63 ± 0.28% for high content (34.8 µg (Fe3O4)/mL). As shown in Table 1 and in accordance with the provided direction for the assessment of biological materials, the INPs generated in this work met the hemolysis test requirements for use as medical materials for blood contact, regardless of the highest doses evaluated.

Iron nanoparticles synthesized by *O. tenuiflorum*	**Concentration micro g mL−1**	**Hemolysis %**
	100	0.01
	150	0.52
	200	1.38
Negative control 10 mM PBS (pH 7.2)		0
Positive control (0.1% sodium carbonate)		100

Table no. 1: Hemolytic activity of INPs synthesized by *O. tenuiflorum*

Toxicity assay

There was no mortality at the recorded concentrations in the control group. The fish showed signs of stress through increasing their swimming activity and attempting to flee the tank. The behavioural stress signals were identical to those mentioned above for iron nanoparticles. Furthermore, when exposed to larger concentrations of iron nanoparticles, the fish in the tank showed increased mucus secretion with strands of sloughed mucus.

Conclusion

Inflammation is associated with many diseases like arthritis, allergies, asthma, cardiovascular disease, chronic obstructive pulmonary disease, diabetes, and psoriasis. The present available anti-inflammatory drugs have many severe side effects, such as dizziness, headaches, fluid retention, indigestion, and adverse problems such as failure of kidney, liver, and heart functions. INPs could be potential anti-inflammatory agents. The significance of this study lies in the easy, fast, cost-effective, and eco-friendly synthesis of INPs with *in vivo* anti-inflammatory activity. This proposal will advance the understanding of the mechanisms in exploring of anti- inflammatory action of INPs, the role of all the phytochemicals of *O. tenuiflorum* leaf extract, and their analysis. Further understanding of the toxicity study will help in improving the process and in vivo application.

REFERENCES

1. Sun SN, Wei C, Zhu ZZ, Hou YL, Venkatraman SS, Xu ZC. Magnetic iron oxide nanoparticles: Synthesis and surface coating techniques for biomedical applications. Chinese Physics B. 2014 Mar 1;23(3):037503.
2. Ali A, Zafar H, Zia M, ul Haq I, Phull AR, Ali JS, Hussain A. Synthesis, characterization, applications, and challenges of iron oxide nanoparticles. Nanotechnology, science and applications. 2016 Aug 19:49-67.
3. Park TJ, Lee KG, Lee SY. Advances in microbial biosynthesis of metal nanoparticles. *Appl Microbiol Biotechnol.* 2016;100:521–534. doi:10.1007/s00253-015-6904-7.
4. Thakkar KN, Mhatre SS, Parikh RY. Biological synthesis of metallic nanoparticles. *Nanomedicine (Lond).* 2010;6(2):257–262.
5. Kumar V, Kaushik NK, Tiwari SK, Singh D, Singh B. Green synthesis of iron nanoparticles: Sources and multifarious biotechnological applications. *Int J Biol Macromol.* 2023;253:127017. doi:10.1016/j.ijbiomac.2023.127017.
6. Gordon MC, David JN. Natural product drug discovery in the next millennium. *Pharm Biol.* 2001;39:8–17.
7. Singh V, Amdekar S, Verma O. Ocimum sanctum (tulsi): Biopharmacological activities. *Webmed Central Pharmacol.* 2010;1(10):1–7.
8. Mirje MM, Zaman SU, Ramabhimaiah S. Evaluation of the anti-inflammatory activity of *Ocimum sanctum* Linn (Tulsi) in albino rats. *Int J Curr Microbiol App Sci.* 2014;3(1):198–205.
9. Umamageswari A, Kudagi BL. Anti-inflammatory and analgesic properties of *Ocimum sanctum*: a comparative study using animal models. *Int J Basic Clin Pharmacol.* 2015;4(5):981–987. doi:10.18203/2319-2003.ijbcp20150878.
10. Gwari A, Negi A, Mishra M. Evaluation of anti-inflammatory activity of tulsi stem (*Ocimum sanctum* Linn.) by using carrageenan-induced paw edema model. *World J Pharm Med Res.* 2021;7(11):272–278.
11. Srichok J, Yingbun N, Kowawisetsut T, Kornmatitsuk S, Suttisansanee U, Temviriyanukul P, Chantong B. Synergistic antibacterial and anti-inflammatory activities of *Ocimum tenuiflorum* ethanolic extract against major bacterial mastitis pathogens. *Antibiotics (Basel).* 2022;11:510. doi:10.3390/antibiotics11040510.
12. Gangopadhyay A, Panda SS, Padmasri B, Panda N. Antioxidant, anti-inflammatory and anthelminthic

activities of traditionally used *Ocimum basilicum* L. and *Ocimum tenuiflorum* L. extract loaded emulsion. *Int J Pharm Qual Assur.* 2024;15(2):706–711.
13. Ahmad T, Phul R, Khatoon N, Sardar M. Antibacterial efficacy of *Ocimum sanctum* leaf extract treated iron oxide nanoparticles. *New J Chem.* 2017;41:2055–2061.
14. Prabhu NN, Kowshik M. Green route synthesis and preliminary characterization of iron oxide nanoparticles using leaf extract of *Ocimum tenuiflorum*. *J Appl Mater Sci Eng Res.* 2019;3:1–5.
15. Panigrahy SK, Singhamahapatra A, Jena M, Sahoo S. Green synthesis of metal nanoparticles using *Ocimum sanctum* (Tulsi). *Int J Pharm Biol Sci.* 2020;10(2):338–349. doi:10.21276/ijpbs.2020.10.2.42.
16. Hirad AH, Ansari SA, Ali MAE, Egeh MA. Microwave-mediated synthesis of iron oxide nanoparticles: photocatalytic, antimicrobial and cytotoxicity assessment. *Process Biochem.* 2022;118:205–214.
17. Periakaruppan R, Ariuthayan B, Vanathi P, Abed SA, Al-Awsi GRL, Al-Dayan N, Dhanasekaran S. *Ocimum tenuiflorum*-assisted fabrication of iron oxide nanoparticles and its use in wastewater treatment of the textile industry. *JOM.* 2023;75(12). doi:10.1007/s11837-023-06076-y.
18. Calder PC, Albers R, Antoine JM, Blum S, Bourdet-Sicard R, Ferns GA, Zhao J. Inflammatory disease processes and interactions with nutrition. *Br J Nutr.* 2009;101(S1):1–45.
19. Schmid-Schönbein GW. Analysis of inflammation. *Annu Rev Biomed Eng.* 2006;8:93–151.
20. Harirforoosh S, Asghar W, Jamali F. Adverse effects of nonsteroidal anti-inflammatory drugs: an update of gastrointestinal, cardiovascular and renal complications. *J Pharm Pharm Sci.* 2013;16(5):821–847.
21. Narendhirakannan RT, Subramanian S, Kandaswamy M. Biochemical evaluation of antidiabetogenic properties of some commonly used Indian plants on streptozotocin-induced diabetes in experimental rats. *Clin Exp Pharmacol Physiol.* 2006;33(12):1150–1157.
22. Cervini-Silva J, Camacho AN, Palacios E, del Angel P, Pentrak M, Pentrakova L, Theng BKC. Anti-inflammatory, antibacterial and cytotoxic activity by natural matrices of nano-iron (hydr)oxide/halloysite. *Appl Clay Sci.* 2016;120:101–110.
23. Agarwal H, Nakara A, Shanmugam VK. Anti-inflammatory mechanism of various metal and metal oxide nanoparticles synthesized using plant extracts: a review. *Biomed Pharmacother.* 2019;109:2561–2572.
24. Moldovan B, David L, Vulcu A, Olenic L, Perde-Schrepler M, Fischer-Fodor E, Filip GA. In vitro and in vivo anti-inflammatory properties of green synthesized silver nanoparticles using *Viburnum opulus* L. fruits extract. *Mater Sci Eng C.* 2017;79:720–727.
25. Agarwal H, Shanmugam V. A review on anti-inflammatory activity of green synthesized zinc oxide nanoparticle: mechanism-based approach. *Bioorg Chem.* 2020;94:103423.
26. Shahid S, Ejaz A, Javed M, Mansoor S, Iqbal S, Elkaeed EB, Nazim Sarwar M. The anti-inflammatory and free radical scavenging activities of bio-inspired nano magnesium oxide. *Front Mater.* 2022;9:875163.
27. Almurshedi AS, El-Masry TA, Selim H, El-Sheekh MM, Makhlof ME, Aldosari BN, El-Bouseary MM. New investigation of anti-inflammatory activity of *Polycladia crinita* and biosynthesized selenium nanoparticles: isolation and characterization. *Microb Cell Fact.* 2023;22(1):173.
28. Zahoor S, Sheraz S, Shams DF, Rehman G, Nayab S, Shah MIA, Khan W. Biosynthesis and anti-inflammatory activity of zinc oxide nanoparticles using leaf extract of *Senecio chrysanthemoides*. *Biomed Res Int.* 2023;2023:3280708.
29. Varghese RM, Kumar A, Shanmugam R. Comparative anti-inflammatory activity of silver and zinc oxide nanoparticles synthesized using *Ocimum tenuiflorum* and *Ocimum gratissimum* herbal formulations. *Cureus.* 2024;16(1).
30. Diallo F, Seck I, Ndoye SF, Niang T, Dieng SM, Thiam F, Seck M. Green synthesis and anti-inflammatory activity of silver nanoparticles based on leaves extract of *Aphania senegalensis*. *Biochem Res Int.* 2024;2024:3468868.
31. Nadagouda MN, Castle AB, Murdock RC, Hussain SM, Varma RS. In vitro biocompatibility of nanoscale zerovalent iron particles (NZVI) synthesized using tea polyphenols. *Green Chem.* 2010;12:114–122.
32. Hanini A, Schmitt A, Kacem K, Chau F, Ammar S, Gavard J. Evaluation of iron oxide nanoparticle biocompatibility. *Int J Nanomedicine.* 2011;6:787–794.
33. Blechinger J, et al. Uptake kinetics and nanotoxicity of silica nanoparticles are cell type dependent. *Small.* 2013;9:3970–3980.
34. Lee J, Lee JH, Lee SY, Park SA, Kim JH, Hwang D, Kim KA, Kim HS. Antioxidant iron oxide nanoparticles: their biocompatibility and bioactive properties. *Int J Mol Sci.* 2023;24:15901. doi:10.3390/ijms242115901.
35. Paima TC, Wermuth DP, Bertacao I, Zanatelli C, Naasani LIS, Slaviero M, Driemeier D, Schaeffer L, Wink MR. Evaluation of in vitro and in vivo biocompatibility of iron produced by powder metallurgy. *Mater Sci Eng C.* 2020;115:111129. doi:10.1016/j.msec.2020.111129.
36. Yang L, Kuang H, Zhang W, Aguilar ZP, Xiong Y, Lai W, Xu H, Wei H. Size-dependent biodistribution and toxicokinetics of iron oxide magnetic nanoparticles in mice. *Nanoscale.* 2015;7:625–636.

37. Patil US, Adireddy S, Jaiswal A, Mandava S, Lee BR, Chrisey DB. In vitro/in vivo toxicity evaluation and quantification of iron oxide nanoparticles. *Int J Mol Sci.* 2015;16:24417–24450. doi:10.3390/ijms161024417.
38. Kumar V, Sharma N, Maitra SS. In vitro and in vivo toxicity assessment of nanoparticles. *Int Nano Lett.* 2017;7:243–256. doi:10.1007/s40089-017-0221-3.
39. Feng Q, Liu Y, Huang J, Chen K, Huang J, Xiao K. Uptake, distribution, clearance and toxicity of iron oxide nanoparticles with different sizes and coatings. *Sci Rep.* 2018;8:2082. doi:10.1038/s41598-018-19628-z.
40. Wu L, Wen W, Wang X, Huang D, Cao J, Qi X, Shen S. Ultrasmall iron oxide nanoparticles cause significant toxicity by inducing acute oxidative stress to multiple organs. *Part Fibre Toxicol.* 2022;19:24. doi:10.1186/s12989-022-00465-y.
41. Zhu X, Tian S, Cai Z. Toxicity assessment of iron oxide nanoparticles in zebrafish (*Danio rerio*) early life stages. *PLoS One.* 2012;7(9):e46286.
42. Hafiz SM, Kulkarni SS, Thakur MK. In vivo toxicity assessment of biologically synthesized iron oxide nanoparticles in zebrafish (*Danio rerio*). *Biosci Biotechnol Res Asia.* 2018;15(2).
43. Sharma A, Karim H, Kaur M, Rathee J, Nandal K, Dahiya P, Shaikh AR. Phytochemical evaluation and biosynthesis of *Ocimum tenuiflorum*-based iron nanoclusters: an integrated experimental and DFT approach. *Results Surf Interfaces.* 2025;19:100494.
44. Kaur M. Impact of response surface methodology-optimized synthesis parameters on in vitro anti-inflammatory activity of iron nanoparticles synthesized using *Ocimum tenuiflorum* Linn. *BioNanoScience.* 2020;10(1):1–10.
45. Gandhidasan R, Thamaraichelvan A, Baburaj S. Anti-inflammatory action of *Lannea coromandelica* by HRBC membrane stabilization. 1991.
46. Brattsand R, Thalén A, Roempke K, Källström L, Gruvstad E. Influence of 16α,17α-acetal substitution and steroid nucleus fluorination on the topical to systemic activity ratio of glucocorticoids. *J Steroid Biochem.* 1982;16(6):779–786.
47. Winter CA, Risley EA, Nuss GW. Carrageenin-induced edema in hind paw of the rat as an assay for anti-inflammatory drugs. *Proc Soc Exp Biol Med.* 1962;111(3):544–547.
48. Kiwumulo HF, Muwonge H, Ibingira C, Lubwama M, Kirabira JB, Ssekitoleko RT. Green synthesis and characterization of iron oxide nanoparticles using *Moringa oleifera*: a potential protocol for use in low and middle income countries. *BMC Res Notes.* 2022;15:149. doi:10.1186/s13104-022-06039-7.
49. Sani DM, Adamu A, Ameta SK, Kura NU. Eco-friendly synthesis and characterization of iron nanoparticles using crude extract from *Eucalyptus globulus* leaves as reducing and capping agents. *Nanochem Res.* 2022;7(2):135–142. doi:10.22036/ncr.2022.02.008.
50. Üstün E, Önbaş SC, Çelik SK, Ayvaz MÇ, Şahin N. Green synthesis of iron oxide nanoparticles using *Ficus carica* leaf extract and its antioxidant activity. *Biointerface Res Biochem.* 2022;12(2):2108–2116. doi:10.33263/BRIAC122.21082116.
51. Aida MS, Alonizan N, Zarrad B, Hjiri M. Green synthesis of iron oxide nanoparticles using *Hibiscus* plant extract. *J Taibah Univ Sci.* 2023;17(1):2221827. doi:10.1080/16583655.2023.2221827.
52. Kumar B, Smita K, Galeas S, Sharma V, Guerrero VH, Debut A, Cumbal L. Characterization and application of biosynthesized iron oxide nanoparticles using *Citrus paradisi* peel: a sustainable approach. *Inorg Chem Commun.* 2020;119:108116. doi:10.1016/j.inoche.2020.108116.
53. Makarov VV, Makarova SS, Love AJ, Sinitsyna OV, Dudnik AO, Yaminsky IV, Taliansky ME, Kalinina NO. Biosynthesis of stable iron oxide nanoparticles in aqueous extracts of *Hordeum vulgare* and *Rumex acetosa* plants. *Langmuir.* 2014;30:5982–5988.
54. De León-Condés CA, Roa-Morales G, Martínez-Barrera G, Balderas-Hernández P, Menchaca-Campos C, Ureña-Núñez F. A novel sulfonated waste polystyrene/iron oxide nanoparticles composite: green synthesis, characterization and applications. *J Environ Chem Eng.* 2019;7:102841. doi:10.1016/j.jece.2018.102841.
55. Rajiv P, Bavadharani B, Kumar MN, Vanathi P. Synthesis and characterization of biogenic iron oxide nanoparticles using green chemistry approach and evaluating their biological activities. *Biocatal Agric Biotechnol.* 2017;12:45–49.
56. Vasantharaj S, Sathiyavimal S, Senthilkumar P, LewisOscar F, Pugazhendhi A. Biosynthesis of iron oxide nanoparticles using leaf extract of *Ruellia tuberosa*: antimicrobial properties and their applications in photocatalytic degradation. *J Photochem Photobiol B.* 2019;192:74–82.
57. Ibe B, et al. Green synthesis of iron oxide nanoparticles using pomegranate seeds extract and photocatalytic activity evaluation for the degradation of textile dye. *J Mater Res Technol.* 2019;8(6):6115–6124. doi:10.1016/j.jmrt.2019.10.006.
58. Wu W, He Q, Jiang C. Magnetic iron oxide nanoparticles: synthesis and surface functionalization strategies. *Nanoscale Res Lett.* 2008;3:397–401. doi:10.1007/s11671-008-9174-9.
59. Niluxsshun MCD, Masilamani K, Mathiventhan U. Green synthesis of silver nanoparticles from the extracts of fruit peel of *Citrus tangerina*, *Citrus sinensis* and *Citrus limon* for antibacterial activities. *Bioinorg Chem Appl.* 2021;2021:6695734. doi:10.1155/2021/6695734.

60. Da'na E, Taha A, Afkar E. Green synthesis of iron nanoparticles by *Acacia nilotica* pods extract and its catalytic, adsorption and antibacterial activities. *Appl Sci.* 2018;8(10).
61. Salem SS, Badawy MSE, Al-Askar AA, Arishi AA, Elkady FM, Hashem AH. Green biosynthesis of selenium nanoparticles using orange peel waste: characterization, antibacterial and antibiofilm activities against multidrug-resistant bacteria. *Life.* 2022;12(6):893.
62. Demirezen DA, Yilmaz D, Yılmaz S. Green synthesis and characterization of iron nanoparticles using *Aesculus hippocastanum* seed extract. *Int J Adv Sci Eng Technol.* 2018;6.
63. Üstün E, Önbaş SC, Çelik SK, Ayvaz MÇ, Şahin N. Green synthesis of iron oxide nanoparticles using *Ficus carica* leaf extract and its antioxidant activity. *Biointerface Res Appl Chem.* 2022;12(2):2108–2116.
64. Meléndrez MF, Cárdenas G, Arbiol J. Synthesis and characterization of gallium colloidal nanoparticles. *J Colloid Interface Sci.* 2010;346:279–287.
65. Duman O, Tunc S. Electrokinetic and rheological properties of Na-bentonite in some electrolyte solutions. *Microporous Mesoporous Mater.* 2009;117:331–338.
66. Nahari MH, Al Ali A, Asiri A, Mahnashi MH, Shaikh IA, Shettar AK, Hoskeri J. Green synthesis and characterization of iron nanoparticles synthesized from aqueous leaf extract of *Vitex leucoxylon* and its biomedical applications. *Nanomaterials.* 2022;12:2404. doi:10.3390/nano12142404.
67. Saranya S, Vijayarani K, Pavithra S. Green synthesis of iron nanoparticles using aqueous extract of *Musa ornata* flower sheath against pathogenic bacteria. *Indian J Pharm Sci.* 2017;79(5):688–694.
68. Sani MD, Adamu A, Ameta SK, Kura NU. Eco-friendly synthesis and characterization of iron nanoparticles using crude extract from *Eucalyptus globulus* leaves as reducing and capping agents. *Nanochem Res.* 2022;7(2):135–142. doi:10.22036/ncr.2022.02.008.
69. Johnson A, Uwa P. Eco-friendly synthesis of iron nanoparticles using *Uvaria chamae*: characterization and biological activity. *Inorg Nano-Met Chem.* 2019;49(12):431–442. doi:10.1080/24701556.2019.1661448.
70. Abdullah JAA, Salah Eddine L, Abderrhmane B, Alonso-González M, Guerrero A, Romero A. Green synthesis and characterization of iron oxide nanoparticles using *Phoenix dactylifera* leaf extract and evaluation of their antioxidant activity. *Sustain Chem Pharm.* 2020;17:100280. doi:10.1016/j.scp.2020.100280.
71. Pindiga NY, Abubakar A, Danbature WL, Muhammae UY. Green synthesis and characterization of iron nanoparticles from the leaf extract of *Khaya senegalensis* (mahogany) and its antimicrobial activity. *Lett Appl Nanobiosci.* 2023;12(3):86. doi:10.33263/LIANBS123.086.
72. Shabbir MA, Naveed M, Rehman SU, Ain NU, Aziz T, Alharbi M, Alsahammari A, Alasmari AF. Synthesis of iron oxide nanoparticles from *Madhuca indica* plant extract and assessment of their cytotoxic, antioxidant, anti-inflammatory and anti-diabetic properties via nanoinformatics approaches. *ACS Omega.* 2023;8:33358–33366. doi:10.1021/acsomega.3c02744.
73. Shende AP, Mitra N. Green synthesis of iron nanoparticles using bioflocculant extracted from okra (*Abelmoschus esculentus* (L) Moench) and its application towards elimination of toxic metals from wastewater: a statistical approach. *J Water Environ Nanotechnol.* 2021;6(4):338–355.
74. Buarki F, AbuHassan H, Al Hannan F, Henari FZ. Green synthesis of iron oxide nanoparticles using *Hibiscus rosa-sinensis* flowers and their antibacterial activity. *J Nanotechnol.* 2022;2022:5474645. doi:10.1155/2022/5474645.
75. Wang J, Witte F, Xi T, Zheng Y, Yang K, Yang Y, Qin L. Recommendation for modifying current cytotoxicity testing standards for biodegradable magnesium-based materials. *Acta Biomater.* 2015;21:237–249.